The design and synthesis of inhibitors of dethiobiotin synthetase as potential herbicides†

Alan R Rendina,[1]* Wendy S Taylor,[1]* Katharine Gibson,[2] George Lorimer‡ Dennis Rayner,[1] Bruce Lockett,[1] Kevin Kranis,[1] Barry Wexler,[1] Dana Marcovici-Mizrahi,§ Ayelet Nudelman,[3] Abraham Nudelman,[3] Eileen Marsilii,[1] Hongji Chi,[1] Zdislaw Wawrzak,[2] Joseph Calabrese,[2] Weijun Huang,[4] Jia Jia,[4] Gunter Schneider,[4] Ylva Lindqvist[4] and Guang Yang[1]

[1] *E.I. Du Pont de Nemours and Co, Stine-Haskell Research Center, Newark, DE 19714, USA*

[2] *E.I. Du Pont de Nemours and Co, Experimental Station, Wilmington, DE 19880, USA*

[3] *Bar Ilan University, Ramat Gan 52900, Israel*

[4] *Karolinska Institute, Stockholm 17177, Sweden*

Abstract: Dethiobiotin synthetase (DTBS; E.C. 6.6.6.6), the penultimate enzyme in the biosynthesis of the essential vitamin biotin, is a new potential target for novel herbicides. Inhibitors were designed based on mechanistic and structural information. The in-vitro activities of these potential inhibitors versus the bacterial enzyme are reported here. Mimics of 7,8-diaminopelargonic acid (DAPA) or the DAPA carbamate reaction intermediate were substrates or partial substrates for the enzyme. Synergistic binding with ATP was noted with compounds which contained an amino functionality. NMR studies and X-ray structures confirmed that the inhibitors could be phosphorylated by the enzyme. Several series of potential inhibitors were designed to take advantage of this partial substrate activity by generating potentially more tightly bound phosphorylated inhibitors *in situ*. Structure–activity relationships for these series based on both substrate and inhibitory activity are described herein. An X-ray structure for one of these inhibitors is also discussed. Although considerable potential for inhibitors of this type was demonstrated, none of the compounds reported showed sufficient herbicidal activity to be a commercial proposition.

Keywords: diamine; diacid; phosphinate; phosphonate; phosphate; diaminopelargonic acid; DAPA; DAPA carbamate; dethiobiotin synthetase; DTBS; biotin biosynthesis; herbicide; inhibition

1 INTRODUCTION

Biotin plays a key role in carboxylation reactions which are critical to microorganisms, animals and plants.[1,2] Thus, the biotin biosynthetic pathway may provide new targets for herbicide design. Biotin is an essential, water-soluble vitamin found in nearly all living cells. Microorganisms, plants and a few fungi make their own biotin, while animals require trace amounts in their diets and most fungi obtain biotin from the environment. Biotin is a covalently attached cofactor that functions as a carbon dioxide carrier in carboxylation, transcarboxylation and decarboxylation reactions.[1,2] Acetyl-CoA carboxylase, the rate-limiting step in lipid biosynthesis in plants, is a biotin-dependent enzyme and a known target for commercial herbicides such as sethoxydim and quizalofop.[3] This enzyme is also a key branch point in plant metabolism because the product, malonyl-CoA, is used for biosynthesis of flavonoids, stilbenoids, naphthoquinones and malonyl aminocyclopropane carboxylic acid, to name a few. Thus, depletion of biotin in plants caused by inhibition of one of the biosynthetic enzymes should result in multiple pleiotropic effects similar to those observed on direct inhibition of acetyl-CoA carboxylase.

The biotin biosynthetic pathway is understood in detail in microorganisms,[4] but is relatively poorly understood in plants. However, there is increasing evidence that plants synthesize biotin using the same route as that in *Escherichia coli* (Mig.) Cast. &

* Correspondence to: Alan R Rendina/Wendy S Taylor, E.I. Du Pont de Nemours and Co, Stine-Haskell Research Center, Newark, DE 19714, USA

E-mail: alan.r.rendina/wendy.s.taylor@usa.dupont.com

† Based on poster presentations at the 9th International Congress of Pesticide Chemistry, organised by the International Union of Pure and Applied Chemistry (IUPAC), and held in London, UK, 2–7 August 1998.

‡ Present address: University of Maryland, College Park, MD 20742, USA

§ Present address: Israel Institute for Biological Research, Ness Ziona 74100, Israel

(*Received 6 July 1998; revised version received 1 October 1998; accepted 19 October 1998*)

Chalm.[5–9] In addition, two biotin auxotrophic mutants have been identified in *Arabidopsis thaliana* Heynh.[7–9] The *bio1* auxotroph has been shown to be defective in 7,8-diaminopelargonic acid (DAPA) synthase[8] and the *bio2* auxotroph is defective in biotin synthase.[9] Both are embryo-defective mutants which fail to grow in the absence of biotin or the appropriate biotin precursor. These studies also indicate that the enzymes of the biotin biosynthetic pathway may be potential new targets for the discovery of environmentally friendly, low use-rate, broad-spectrum herbicides.

Dethiobiotin synthetase (DTBS; E.C. 6.6.6.6) catalyzes the penultimate step in biotin synthesis, the formation of the ureido ring of DTB from (7*R*), (8*S*)-DAPA, CO_2 and ATP (Fig 1).[10] *E. coli* DTBS has been overexpressed[11–14] and the reaction mechanism[10,13–20] and X-ray crystal structure[11,12,14,15,17,18,20] have been studied and described in earlier papers. The goal of the work presented here was to use the mechanistic information to design inhibitors of the enzyme and to test the inhibitors for herbicidal activity. In the absence of a practical source of the plant enzyme (no plant sequences have been reported to date, and we have been able to detect only very small amounts of activity in plant tissues using a highly sensitive radiochemical assay; Rendina AR & Gibson KJ, unpublished), we used the bacterial enzyme as a model.

At pH 7.5 substrate K_M values are in the micromolar range, being 0.4, 0.3 and 4 μM for ATP, DAPA and CO_2, respectively. In contrast, K_i values are greater for the products, ie >1 mM for dethiobiotin and inorganic phosphate (Pi) and 14 μM for ADP.[13,21] DAPA and ATP appear to bind in synergistic fashion, whereas the concentration of CO_2 does not affect the apparent K_M of DAPA or ATP.[13,21] Random addition of substrates[21] was confirmed by pulse-chase experiments which showed that both preformed E*DAPA*CO_2[13] and E*MgATP (Gibson KJ, unpublished) complexes were committed to form products. Since the K_M values for the reactants were low, initial inhibitor design strategies focused on the preparation of mimics of the substrate and of the DAPA carbamate. Subsequent inhibitor design focused on the preparation of DAPA carbamate mimics which could become phosphorylated by the enzyme *in situ* to generate a potentially more tightly bound inhibitor. Direct mimics of the phosphorylated DAPA carbamate and postulated tetrahedral intermediate (Fig 1) are not covered in this discussion and were deliberately avoided in initial design strategies due to potentially poor uptake and translocation properties of such highly charged molecules and to potential problems arising from competition with high intracellular concentrations of ATP. Preliminary reports of this work have been presented elsewhere.[21,22]

Table 1. Substrate activity of DAPA analogs (structures shown in Fig 3)[a]

Compound	*Rel. V_{max}*(%)	*K_m* (μM)	*Rel. V_{max}/K_M*(%)
1	100	1.3	100
2	32	14	3
3	10	2000	0.006
4	74	1900	0.05
5	216	8600	0.033
6	—	—	0.0064
7	6.4	1470	0.006
8	1.5[b]	—	—
9	150	15.4	13

[a] Relative V_{max} and V_{max}/K_M values may be inaccurate for the weaker substrates since K_M for ATP and CO_2 may be higher and may not be saturating under the assay conditions (eg K_M for CO_2 at 10 mM **3** is 0.7 mM, compared to 0.004 mM with DAPA as the substrate).
[b] Highest level of **8** was 4 mM; no K_M determined.

2 EXPERIMENTAL METHODS

Compounds **3** and **10–15** (Tables 1–3) were obtained from Aldrich or Sigma. DAPA was prepared as described previously.[13] Synthetic methods for other compounds are outlined at the appropriate point in Section 3 (See Figs 2, 5, 7–12). Details and spectroscopic data for several of the DAPA and DAPA carbamate analogs including those labeled with ^{13}C

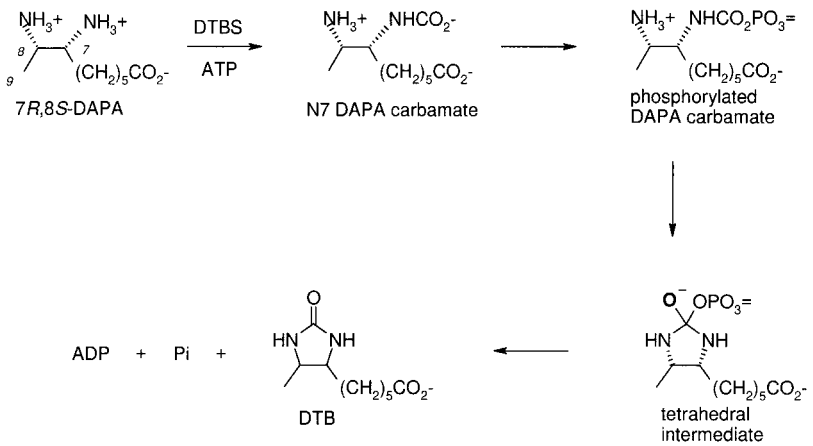

Figure 1. Reaction and proposed mechanism of DTBS.

Table 2. Inhibition and substrate activity of unsubstituted diacid analogs of DAPA carbamate

		$HO_2C(CH_2)_nCO_2H$				
Compound	*n*	K_i (*low ATP*) (μM)	K_i (*high ATP*) (μM)	K_M (μM)	*Rel V* (%)	*Rel V/K* (%)
10	10	8	—	210	1.1	0.01
11	9	7	—	240	11	0.06
12	8	22	—	107	19	0.2
13	7	16	90	90	64	1.0
14	6	70	548	590	12	0.03
15	5	1300	—	7300	6.9	0.001

have been published previously.[13,23–25] Spectroscopic evidence for the remaining compounds prepared for this study is consistent with the structures shown. Methods for obtaining [^{13}C] and [^{31}P]NMR spectra are described elsewhere.[13] DTBS-catalyzed reactions for a typical NMR experiment used to detect new products with alternate substrates contained HEPES buffer, (100 mM; pH 7.8), $MgCl_2$ (7 mM), ATP (3 mM), phosphoenolpyruvate (2 mM), compound (2 mM), pyruvate kinase (5 units; Sigma), DTBS (27 μM) and water containing D_2O (25% by volume). X-ray crystallographic conditions used to solve the structure of compound **38** and MnATP with DTBS are similar to those described previously.[15] Details of the crystallography will be published elsewhere.

Cloning, expression, purification and assays of *E. coli* DTBS were conducted according to published procedures.[13,14] Coupled spectrophotometric assays for either ADP or Pi were the primary tools used for evaluation of substrate activity and inhibition. For substrate activity, varying amounts of each compound were evaluated at pH 7.5 in solutions containing $MgCl_2$ (5 mM), ATP (3 mM) and $NaHCO_3$ (15 mM). The bicarbonate was required for diamines and monoamines, but not for substrate activity of carbamate mimics where acid functionality replaced the carbamate carboxyl group. A radiochemical assay

Table 3. Inhibition and substrate activity of N7-DAPA carbamate mimics

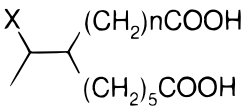

Compound	*X*	*n*	K_i (low ATP) (μM)	K_i (*high ATP*) (μM)	K_M (μM)	*Rel V* (%)	*Rel V/K* (%)
16	NH_3^+	0	70	55	900	80	0.18
17	Keto	1	60	1890	2000	22	0.014
18	OH	1	15	3.3	160	3.8	0.032
19	NH_3^+	1	21	—	4	255	83
20	Keto	2	84	—	940	9	0.01
21	OH	2	50	2620	43	16	0.48
22	NH_3^+	2	124	—	38	34	1.2
23	Keto	3	76	—	—	0.6	—
24	OH	3	100	—	3040	7	0.003
25	NH_3^+	3	770	—	650	19	0.04

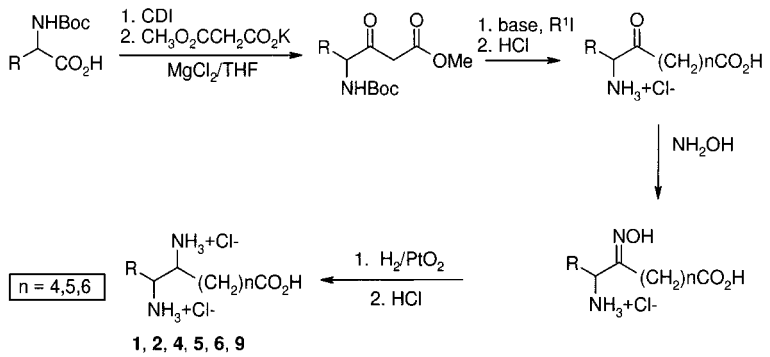

1, 2, 4, 5, 6, 9

Figure 2. Synthesis of diamino acids.

for fixation of $^{14}CO_2$ into acid-stable material was used to detect very weak diamine substrates.[13] Maximal velocities (V_{max}) and V_{max}/K_M values are reported as relative percentages of the activity observed with the natural, chiral substrate, (7*R*), (8*S*)-DAPA. K_i values were calculated from I_{50} determinations conducted at two different ATP levels assuming competition with DAPA and a K_M for DAPA of 1.2 μM (calc $K_i = I_{50}$ $\{K_M/(K_M + [DAPA])\}$. The low ATP K_i was determined at pH 7.5 in solutions containing DAPA (2 μM), ATP (1 μM), $MgCl_2$ (1 mM) and $NaHCO_3$ (3 mM). The high ATP K_i was determined at pH 7.5 in DAPA (2 μM), ATP (3 mM), $MgCl_2$ (5 mM) and $NaHCO_3$ (15 mM). Competition versus DAPA for several inhibitors was confirmed by initial velocity kinetic analysis (data not shown). The phytotoxicity of the compounds was determined by rating the effects visually after germination relative to untreated controls, of doses of 0, 1, 10 and 100 mg litre^{-1} applied to the agar prior to germination of *Arabidopsis thaliana* seedlings.[26,27]

3 RESULTS AND DISCUSSION

3.1 Mimics of DAPA

A variety of diamino acids and monoamino acids was prepared (Fig. 2) and assayed for substrate activity. The structure–activity relationships of these compounds (shown in Fig 3 and Table 1) provided information that was used for the subsequent design of inhibitors. The optimal chain length for substrate activity (relative V_{max}/K_M) for the structures in Fig 3 was the same as is found in the natural substrate **1**; reducing or increasing the chain length decreased the relative V/K_M. The decreased substrate activity of compound **9** (about 10-fold in V/K_M) demonstrates the importance of the 9-methyl group, consistent with the small hydrophobic pocket surrounding this group as seen in the X-ray crystallographic models for DAPA bound to the active site.[15] Both *cis*- and *trans*-cyclohexanediamine were also found to be very weak substrates (relative $V/K_M = 0.001\%$), while 2,3-diaminopropionic acid, 3,4-diaminobenzoic acid, 1,2-phenylenediamine and 4,5-diamino-6-hydroxy-

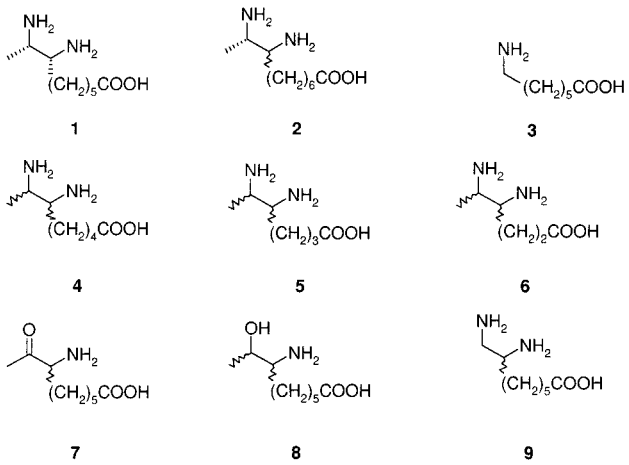

Figure 3. Structures of compounds reported in Table 1.

pyrimidine were not active as substrates (data for these commercially available compounds are not shown in Fig 3 or Table 1). In all cases shown in Table 1, except compounds **3, 7** and **8**, cyclization was observed to form the ureido ring based on the release of P_i and the formation of acid-stable products in the presence of $^{14}CO_2$. The partial substrate activity of the monoamines, **3, 7** and **8**, depended on the presence of CO_2 and was limited to compounds with a six-carbon spacer between the amine and the acid. This partial substrate activity of the monoamines was confirmed using NMR analysis of the enzymatic reaction of compound **3** with [^{12}C] or [^{13}C] $NaHCO_3$. The [^{13}C] and [^{31}P]NMR spectra showed the appearance of a new ^{13}C resonance (156.6 ppm, J = 4.7 Hz) and a new ^{31}P resonance (2.8 ppm, J = 4.9 Hz) which corresponded to the phosphorylated carbamate of monoamine **3** (Fig 4). The lack of substrate activity for 8-aminooctanoic acid and 6-aminohexanoic acid (data not shown) compared to 7-aminoheptanoic acid (compound **3**), is also consistent with the observations on monoamines (see above) and with earlier publications on the enzyme's regioselectivity for the N7-DAPA carbamate.[13]

3.2 Inhibitors based on mimics of the DAPA carbamate

A series of simple, commercially available compounds was assayed as examples of compounds which mimic the N7-DAPA carbamate, but did not have a substituent in the position equivalent to the 8-amine or 9-methyl groups of DAPA (Table 2). The optimal chain length for substrate activity was 9, the same number of atoms as between the two acids of the N7-DAPA carbamate. The optimal chain length for inhibition at subsaturating ATP levels is 11, suggesting that one of the acids overlaps the γ-phosphate site of ATP and picks up extra binding interactions. Unlike the natural substrate, these compounds were not synergistic with ATP, but rather were antagonistic. Observation of the enzymatic reaction with compound **13**, azelaic acid, using [^{31}P]NMR showed that these diacids are partial substrates for DTBS. A new ^{31}P resonance was apparent at −3.07 ppm (Pi had a resonance at 1.22 ppm). The products, acyl-phosphate and MgADP, are released by the enzyme. The acyl-phosphate products can also be converted to Fe^{3+}-hydroxamates in the presence of ferric chloride and hydroxylamine (data not shown). Release of inorganic phosphate with these compounds was not detected using a coupled assay for Pi.

These straight-chain analogs were all poor inhibitors of the enzyme, indicating that the substituents on the C8 of DAPA have important binding contacts consistent with the crystallographic studies of the active-site interactions of DAPA and the N7-DAPA carbamate with the enzyme.[15] The methylene groups can be replaced by double bonds in this series (eg

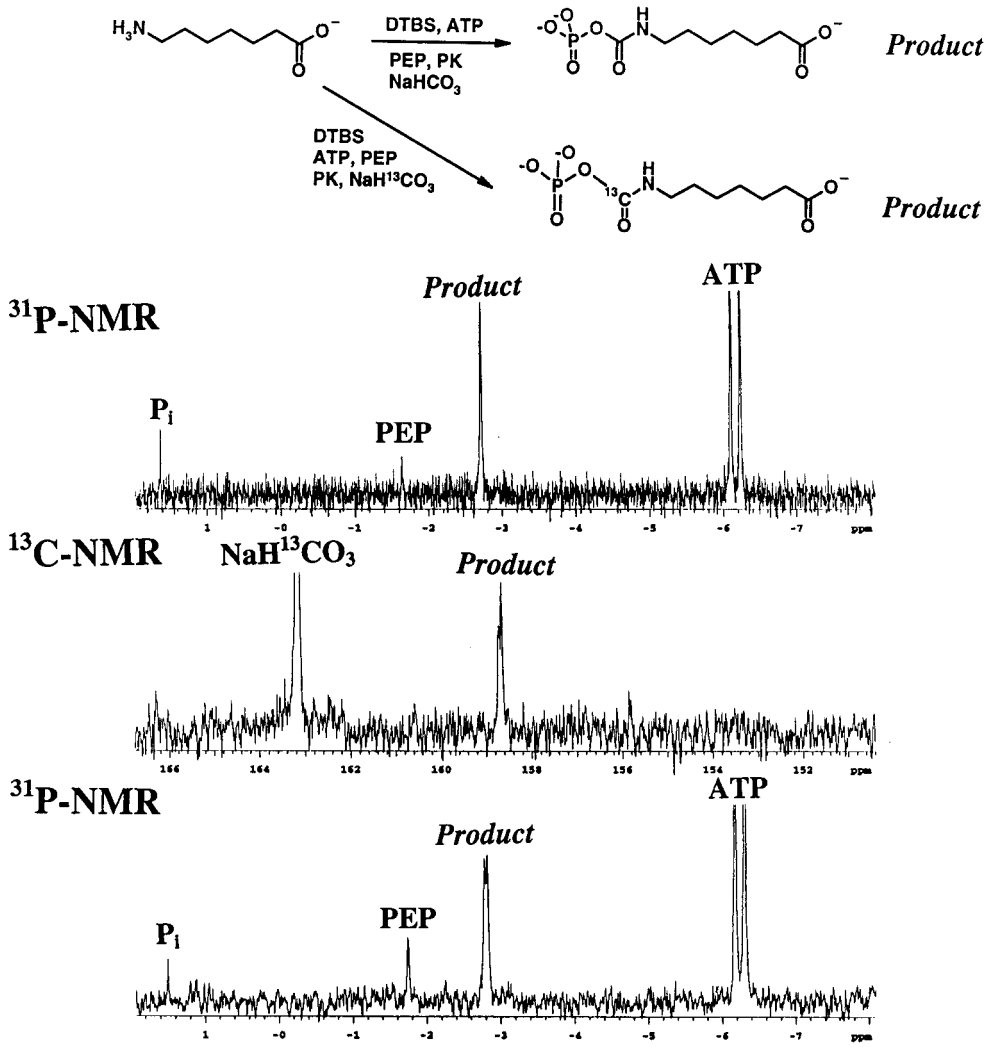

Figure 4. NMR spectra of the enzymatic product produced from compound **3**. Top spectrum: 7-aminoheptanoic acid with unlabeled bicarbonate; middle and bottom spectra: 7-aminoheptanoic acid with [^{13}C-]bicarbonate.

trans traumatic acid is a weak partial substrate; data not shown), but no improved inhibition is obtained. The binding pocket for the alkyl side-chain of DAPA can accommodate an aromatic ring in place of two to four of the methylene groups, but the K_M values are high, the relative V/K_M values are very low compared to other substrates, and the inhibition is weak at high ATP levels (data not shown). Compounds with $n = 7$ and where one of the carboxylic acids was replaced with an alcohol, aldehyde, ester or lactone moiety were very weak inhibitors and had no substrate activity (data and structures not shown). These results indicate that two acid functional groups are needed to mimic the N7-DAPA carbamate and are consistent with the strong H-bonding network around C1 of DAPA observed in the crystal structures.[15]

A series of compounds were prepared as shown in Fig 5 which more closely mimicked the N7-DAPA carbamate by incorporating an extra side-chain in the C7 position of the diacid. The substrate and inhibitory activities of these compounds are summarized in

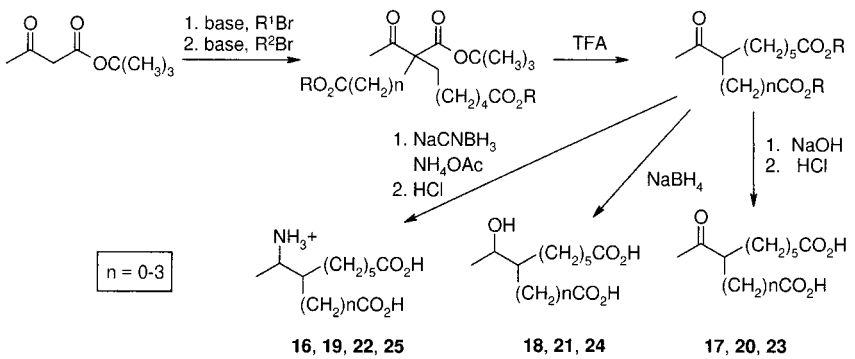

Figure 5. Synthesis of N7-DAPA carbamate analogs.

Table 4. Substrate and inhibitory activity of N7-DAPA carbamate mimics (non-cylizable)

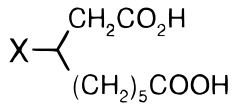

Compound	*X*	*K_i (low ATP)* (μM)	*k_i (high ATP)* (μM)	*K_M* (μM)	*Rel V* (%)	*Rel V/K* (%)
26	Cyclobutyl	3.5	23	32	3.3	0.13
27	Methyl	14.4	1250	495	29	0.08
28	Propyl	10.5	270	250	13	0.07
29	Isopropyyl	9	150	195	7.2	0.05
30	2-Propenyl	9	120	120	5	0.05
31	Phenyl	18	2800	1100	9.4	0.01
32	2-Pyrrole	91	49	45	4.8	0.004
33	3-Pyridyl	70	6300	2420	3.5	0.001
34	$CH(CH_3)NHC(=NH_2^+)NH_2$	350	140	140	84	0.8

Table 3. (K_i values were difficult to determine for these compounds due to the high substrate activity, ie rapid release of ADP. The radiochemical assay was used in place of the ADP-coupled assay for many of these compounds, especially at high ATP.)

The optimal substrate activity was observed for compound **19** when $n = 1$ and $X = NH_3^+$. Longer derivatives ($n = 2$ and 3) showed weaker substrate activity and weaker inhibition at both high and low ATP. NMR experiments with ^{13}C-labeled compound **19** showed that this compound rapidly cyclized in the enzymatic reaction to form the corresponding lactam (Fig 6). The new peaks observed in the experiment corresponded to the spectra obtained from the synthetically prepared lactams.[13] No new ^{31}P signals were observed nor was Pi detected by coupled assay. Interestingly, [^{31}P] and [^{13}C]NMR experiments with unlabeled and ^{13}C-labeled **18**, and concomitant release of ADP and Pi, showed that compound also to give a cyclized product (the lactone shown in Fig 6). The cyclization of either ^{13}C-labeled compound shown in Fig 6 proceeded on all four diastereomers of the substrate, although the rates varied. The highest rate was observed for one of the *erythro* isomers; the lowest rate was for the remaining *erythro* isomer. This indicates that DTBS prefers the stereochemistry of the natural substrate and does not exhibit a strong preference at the 8-position, but does show a preference at the 7-position. The ^{31}P and ^{13}C experiments for ^{13}C-labeled compound **17** where X = keto and $n = 1$ show that partial substrate activity occurs to release an acyl-phosphate (^{31}P resonance at -2.94 ppm, $J = 8.6$ Hz and ^{13}C resonance at 173.2 ppm, $J = 8.5$ Hz) and MgADP, but not Pi; a cyclized product is not formed in this case. Compound **16** also does not appear to cyclize, as ADP is released but not Pi.

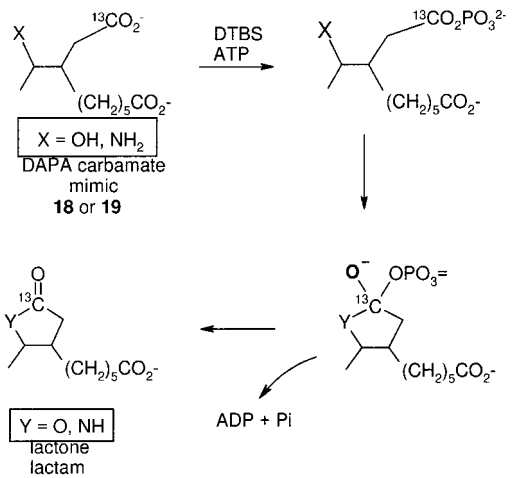

Figure 6. Substrate activity of two carboxylic acid mimics of the N7 DAPA carbamate.

At the optimal chain length the inhibitors shown in Table 3 were better inhibitors than the corresponding straight-chain analogs in Table 2, but the high substrate activity reduced their efficacy since the cyclized products are readily released from the enzyme. The main advantage of the compounds with substituents at the 7-position (ie the X group shown in Table 3) was that they began to show synergistic behavior with ATP, especially when $n = 0$ or 1.

Some additional analogs of the compounds shown in Table 3 were prepared where X was a non-nucleophilic functionality. These analogs, prepared using known methods, could not undergo an enzyme-catalyzed cyclization. It was hoped that these compounds would remain tightly bound to the enzyme after phosphorylation in the active site. These compounds, shown in Table 4, were only partial substrates for DTBS since NMR confirmed that they become phosphorylated, but do not cyclize or release Pi. For example, ^{13}C-labeled compound **26** in the presence of DTBS and ATP produced a new ^{31}P resonance at -3.17 ppm ($J = 8.9$ Hz) and a new ^{13}C resonance at 175.7 ppm ($J = 8.9$ Hz) corresponding to the acyl-phosphate.

Other functional groups such as aldehydes, acids, diols, hydroxamates and oximes could also replace the N8 amine and the C8 methyl group of DAPA but were weakly bound (data and structures not shown). As observed with other series of carbamate mimics, synergy with ATP (in these cases stronger inhibition at high ATP) appears to depend on the presence of a cation or H-bond donor in the 8-position (see the pyrrole of compound **32** and the guanidinium group of compound **34**). Unfortunately, despite the synergy with ATP, these compounds are still relatively weak inhibitors and the phosphorylated products are rapidly released. When the H-bond donor group is an OH or an amino group both synergy and potency occur, but the cyclized products are also rapidly released resulting in substrate activity rather than potent enzyme-activated inhibition. None of the compounds discussed in this section was herbicidal below 10 mg litre^{-1} in the agar-based assay with *A. thaliana*, nor did they affect germination.

3.3 Phosphorus-based mimics of DAPA carbamate

An approach to inhibitor design that has been used successfully for glutamine synthetase,[28–32] D-alanine : D-alanine ligase,[33,34] glutathione synthetase[35] and γ-glutamylcysteine synthetase[36] is to prepare a substrate mimic which can be phosphorylated by the enzyme *in situ* to generate a more tightly bound inhibitor. The carboxylic acid substrate mimics discussed previously did become phosphorylated but did not generate a more tightly bound inhibitor. Analogs with a nucleophilic group on C8 underwent a cyclization reaction. Analogs which could not cyclize were simply released from the enzyme. Another series of inhibitors were prepared which were more closely modeled on phosphinothricin, the known inhibitor of glutamine synthetase, which becomes more tightly bound after it is phosphorylated *in situ*. This series used a phosphorus acid as a mimic for the carbamate group on the N7-DAPA carbamate and varied the chain length, charges, and the side chain. Since the N–P bond is relatively weak, cyclization of amino-substituted analogs should not occur as readily as in the carboxylic acid series. The syntheses of the amino, keto and hydroxyl phosphinate and phosphonate analogs are shown in Fig 7. The phosphinic acid, **36**, and phosphonates **37** and **39** were mixtures of two pairs of diastereomers, whereas the phosphinic acid **38** was a mixture of three pairs of diasteriomers. One of the diastereomers of compound **38** was separated from the remaining mixture of diastereomers. The data for this single isomer are presented in Table 5, but the activity of the mixture of diastereomers was much the same as that of the single diastereomer. The stereochemistry of the single diastereomer was not determined, although it could be deduced from the crystal structure (see Fig 14).

The syntheses of the corresponding amino, hydroxy and alkyl substituted phosphates and phosphonates are shown in Figs 8–10. Chiral (*L*)-alanine was used in the syntheses shown in Fig 8. Racemic lactic acid was used in the synthesis in Fig 9. (Compound **43** was also prepared from (*S*)-lactic acid. The diastereomeric mixture obtained from (*S*)-lactic acid was less potent than the mixture of four diasteriomers obtained from racemic lactic acid.) Compounds **40–45** were mixtures of diastereomers. Compounds **40–43** tended to be slightly labile under acidic conditions and were stored as the sodium salts. Synthetic routes to extended and shortened versions of these inhibitors are shown in Figs 11 and 12. Compounds **47**, **48**, **50**, **53** and **54** were mixtures of two diastereomers. Compound **51** was a mixture of three diastereomers.

A number of interesting comparisons can be made with these phosphorus-based inhibitors (see Table 5). The carbamate binding site in DTBS is in close proximity to the binding site for the γ-phosphate of

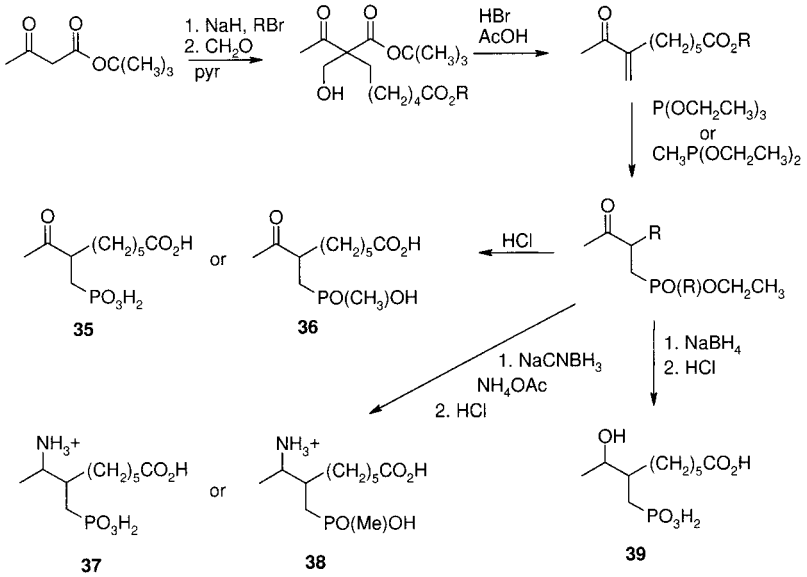

Figure 7. Synthesis of amino, keto and hydroxyl phosphinic and phosphonic analogs.

Compound	K_i (*low ATP*) (μM)	K_i (*high ATP*) (μM)	*Rel V* (%)	*Rel V/K* (%)
35	31	—	25	0.01
36	380	8500	3.6	0.002
37	1.8	45	2.9	0.03
38	121	55	0.8	—
39	10.9	2040	28.7	0.008
40	26	175	0.4	—
41	77	24	—	—
42	56	110	0.5	—
43	0.8	1400	1	—
44	25	1300	—	—
45	5.4	6850	1	—
46	1.7	1300	1	—
47	23	3500	1.2	<0.001
48	1.6	1900	0.3	<0.001
49	7.6	—	1	<0.001
50	71	296	0.4	—
51	190	1700	11.2	0.002
52	59	2500	—	—
53	36	1320	2.7	0.001
54	3.1	2400	1.0	—

Table 5. In-vitro comparison of phosphorus-based inhibitors

ATP. Most of the phosphorus-based inhibitors did not bind synergistically with ATP (K_i at low ATP $< K_i$ at high ATP), suggesting that the phosphorus-containing group was often overlapping the position where ATP normally binds. Only the two analogs **38** and **41** bound synergistically with ATP. These compounds both have phosphorus monoanions and both have an amino group on the side chain. In the pre-

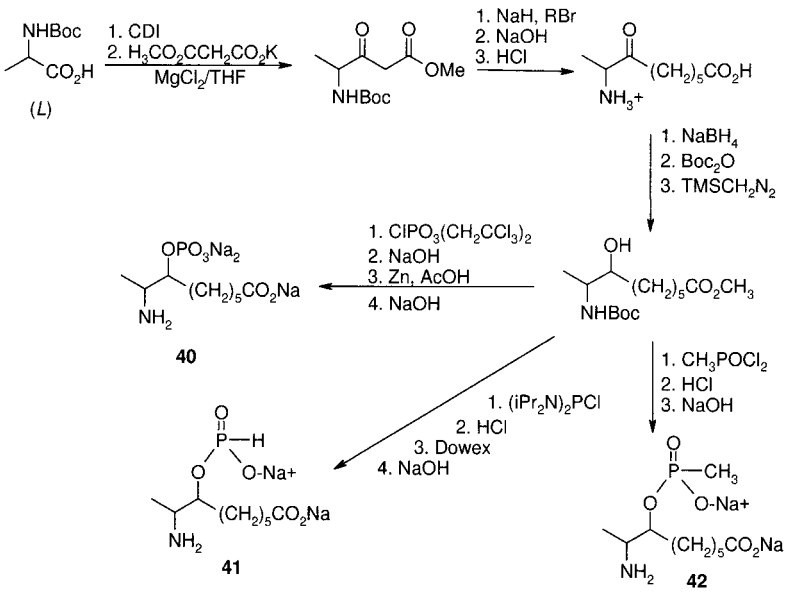

Figure 8. Synthesis of amino-substituted phosphonate and phosphate analogs.

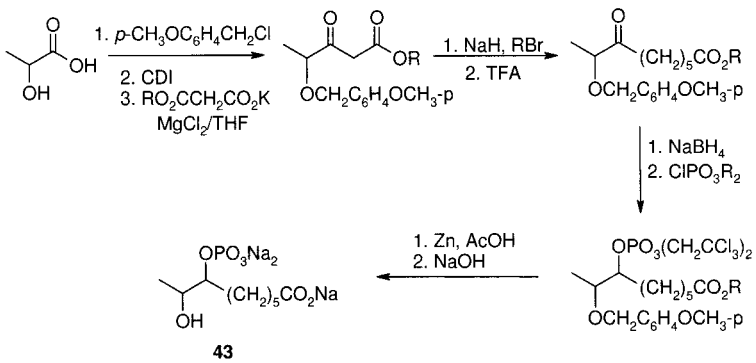

Figure 9. Synthesis of the hydroxyl-substituted phosphate **43**.

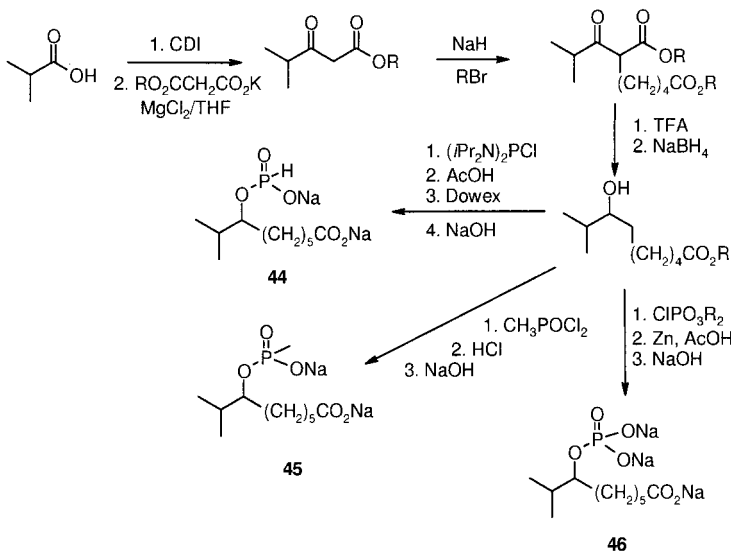

Figure 10. Synthesis of alkyl-substituted phosphates and phosphonates.

vious series of analogs, the amino group was also critical for synergistic binding. A comparison of **44** (amine replaced with a methyl group) with **41** shows that **44** is $>50\times$ less tightly bound at high ATP. A comparison of **41** with **40** and of **38** with **37** shows that the compounds with phosphorus dianions do not bind synergistically with ATP in contrast to the compounds with phosphorus monoanions.

The analogs with an oxygen in the position that corresponds to the N7 position of DAPA were prepared in an attempt to pick up additional binding interactions with Ser-41 (see Fig 14). (Analogs with N–P bonds were not prepared due to their lability.) Mutagenesis studies later showed that Ser-41 has very little effect on the binding or turnover of DAPA, despite being within H-bonding distance of N7 of DAPA.[14] Analysis of the phosphorus-containing inhibitors shows that an increase in potency can occur, but not always, when there is an oxygen in this position. In the case of the phosphonate **39** and the phosphate **43,** the phosphate binds more tightly. However, in the case of the phosphonate **37** and the phosphate **40**, the phosphate binds less tightly.

Although **38** and **41** bound synergistically with ATP, they had very poor substrate activity, indicating that the γ-phosphate was not being transferred efficiently to the inhibitor. The lack of substrate activity could be a desirable attribute if it were accompanied by tighter binding over time and slow release of the ADP and phosphorylated inhibitor products. However, these compounds exhibited no time-dependent increase in potency and were relatively weak inhibitors (μM). Shortened analogs, **50–54** (Fig 12), were prepared in an attempt to decrease the repulsion between the inhibitor and ATP and thereby increase the phosphorylation of the inhibitor. Unfortunately, the shortened versions did

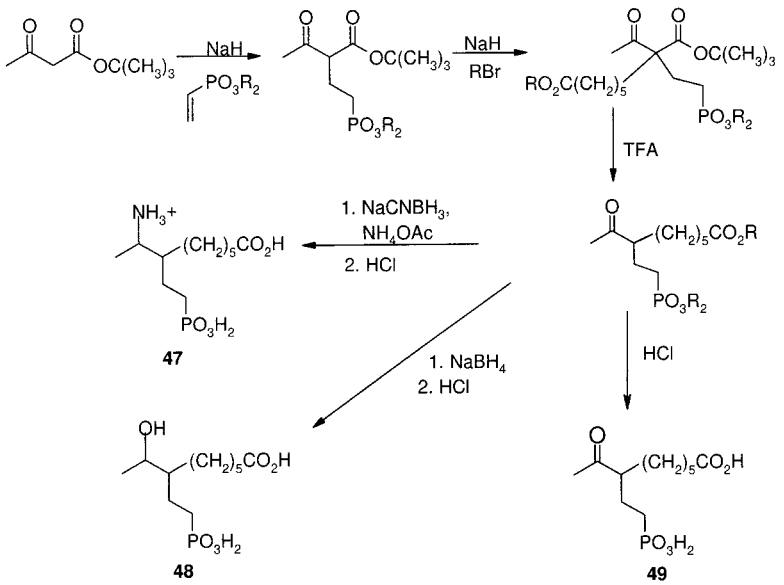

Figure 11. Synthesis of extended phosphonate analogs.

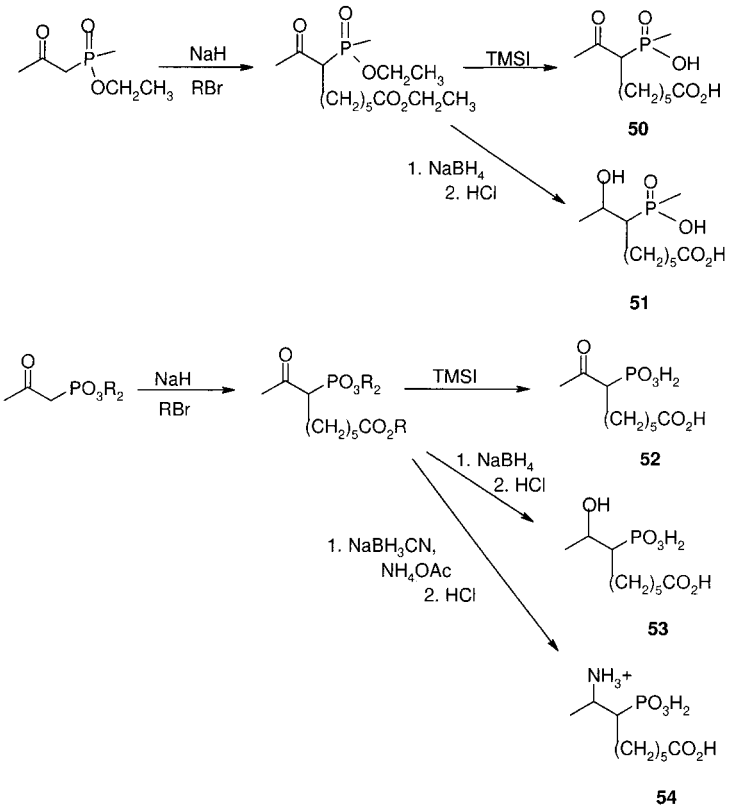

Figure 12. Synthesis of shortened analogs.

not bind synergistically with ATP; in fact antagonism was observed. One possible explanation is that the position of the C8 substituent may dictate where the phosphorus-containing moiety is situated in the active site. For comparison, three longer analogs were prepared (**47–49**) (Fig. 11). Not unexpectedly they showed 150- to >1000-fold increases in K_i at the higher level of ATP. In fact, these longer derivatives could be considered to be mimics of the phosphorylated carbamate.

Although compound **38** was a very poor substrate for the enzyme, when the compound was put with the enzyme under crystallization conditions (mM levels of enzyme and ligands) in the presence of ATP, transfer of phosphate occurred (Fig 13) and the crystal structure was found to contain the phosphorylated product shown in Fig 14. Not surprisingly, the crystal structure of phosphorylated **38** is remarkably similar to that of the actual phosphorylated substrate intermediate recently reported using kinetic crystallography techniques.[20] In Fig 14 the ATP analog, ACP [adenylyl (β,γ-methylene) diphosphonate], was extracted from the crystal structure of DTBS-ACP-**19** (thin line) and superimposed on the crystal structure of DTBS-ADP-phosphorylated **38**. The positions of the γ-phosphate of ACP and of the transferred phosphate are very close to each other and very little movement is required to transfer the phosphate to **38**. Very little change is observed in the orientation of the amino acid sidechains near the active site. DAPA carbamate and the phosphorylated inhibitor are stabilized by interactions with Lys-37 and Ser-41 at the amino end, and by an interaction with Tyr-187 and a network of H-bonds to tightly bound water molecules at the C-1 end. The transferred phosphorus also has interactions with Thr-11, Lys-15 and two metal ions similar to the interactions observed for the inert ATP analog, ACP, and to the phosphorylated substrate intermediate.[15,20] The 8-amino group in DAPA and the inhibitors is within hydrogen bonding distance of the γ-phosphate of ATP. No other major interactions with the amine are observed. The amine is very close to the surface of the enzyme and exposed to water. The exposed nature of the active site may account for the lack of potent binding of the phosphorylated inhibitors. Another reason for either the lack of potency or time-dependent behavior is that, unlike the other four enzymes where this inhibitor strategy was successful, the nucleophilic amino group that attacks the acyl-phosphate (or carbamyl-phosphate) intermediate is intramolecular for DTBS versus intermolecular for the other enzymes. The intramolecular reaction catalyzed by DTBS (expected to be more facile chemically) does not require the amine-

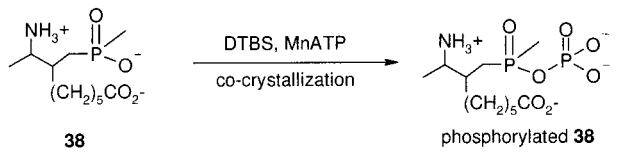

38 phosphorylated **38**

Figure 13. Reaction of **38** with ATP under X-ray crystallization conditions.

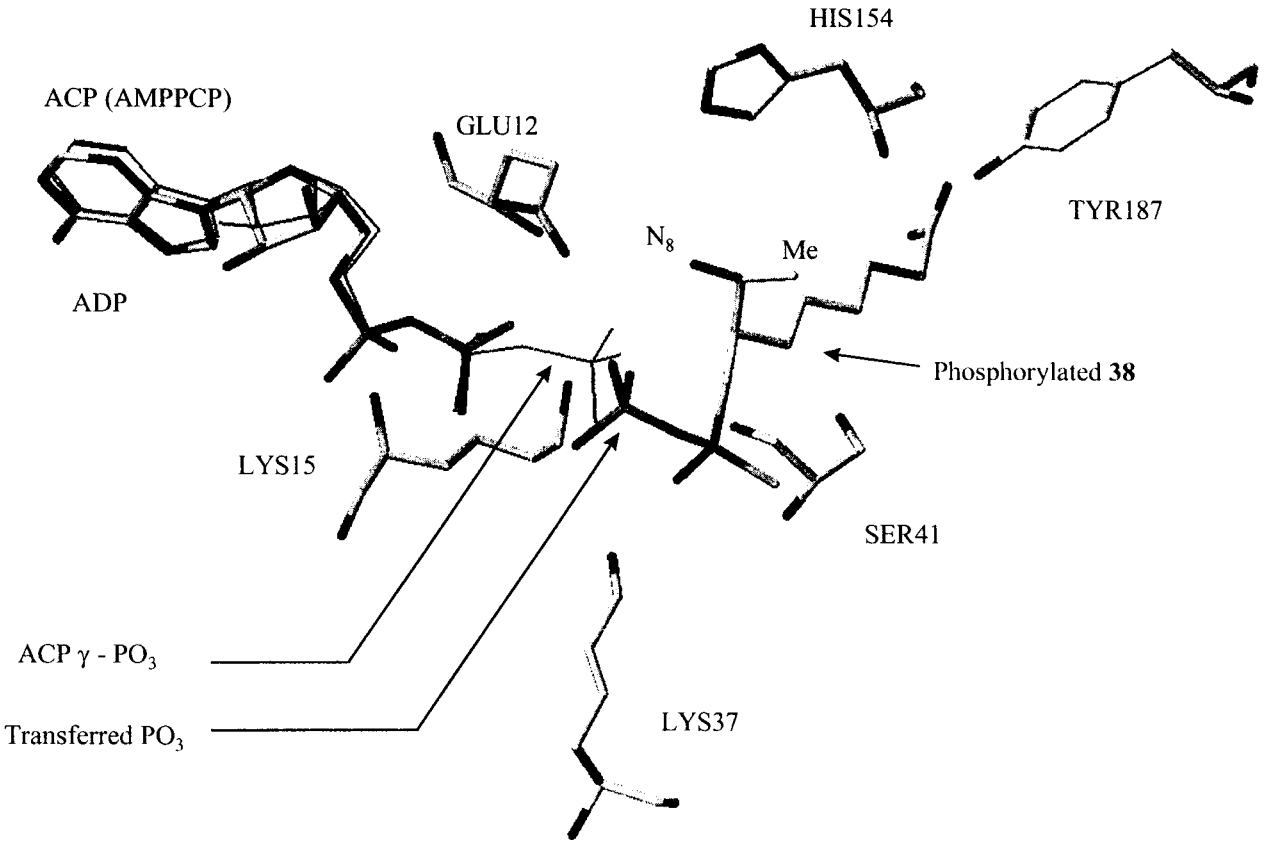

Figure 14. X-ray structure of phosphorylated **38** superimposed with the E-DAPA-CO_2^-ACP structure (thin line). Thr-11 and the two Mn^{2+} atoms found in the structure of phosphorylated **38** near the transferred phosphate are not shown for purposes of clarity.

containing second substrate to be bound tightly and positioned properly, as is required and observed for the other four enzymes.

4 CONCLUSIONS

Amino acids and diacids were good mimics of the DAPA substrate and of the DAPA carbamate intermediate. Low micromolar levels of inhibition were observed. Dianionic phosphorus-based inhibitors which mimicked the DAPA carbamate were generally less potent than monoanionic phosphorus-based inhibitors. The amine in the C-8 position was critical for synergistic binding with ATP in both the phosphorus-containing inhibitors and the carboxylic inhibitors.

The design strategy used for glutamine synthetase (and other enzymes) inhibitors was not successful in this case, perhaps due to the solvent accessibility of the DTBS active site. The carboxylic acid inhibitors which became phosphorylated *in situ* did not remain bound to the active site. The phosphorus-containing inhibitors were very poor partial substrates for DTBS and the amount of phosphorylated inhibitor that was generated was very slight. Unfortunately, none of the inhibitors discussed was a time-dependent inhibitor, nor did any show significant herbicidal activity against *A. thaliana* below 10 mg litre^{-1}.

Whether DTBS and the other enzymes in biotin biosynthesis are good targets for herbicide discovery remains an open question. Future plans include continuation of the search for the plant equivalents to the bacterial enzymes, mostly through the efforts of public and private sector genomic sequencing projects. Once the plant genes and enzymes are obtained, both screening and design approaches to inhibitor discovery can be pursued more confidently; eg knowledge acquired from the bacterial model can be used to design the next generation of inhibitors that exploit binding pockets unique to the plant enzyme.

ACKNOWLEDGEMENTS

We thank colleagues at Dupont who have participated in the dethiobiotin synthetase project, especially Dennis Flint for getting us all started and for many helpful discussions, Vern Wittenbach and Pete Teaney for all the phytotoxicity studies with *A. thaliana*, and Forrest Chumley, Russ Bellina, Mark Nelson and John Pierce for constructive criticism and project support.

REFERENCES

1 Dakshinamurti K and Bhagavan NH (eds), Biotin. *Ann NY Acad Sci*, **447**:1–441 (1985).
2 Knowles JR, The mechanism of biotin-dependent enzymes. *Annu Rev Biochem* **58**:195–221 (1989).
3 Rendina AR, Craig-Kennard AC, Beaudoin JD and Breen MK, Inhibition of acetyl-coenzyme A carboxylase by two

classes of grass-selective herbicides. *J Agric Food Chem* **38**:1282–1287 (1990) and references therein.
4 Eisenberg M, Biosynthesis of biotin and lipoic acid, in *Escherichia coli and Salmonella typhimurium – Cellular and Molecular Biology*, ed by Neidhardt F, American Society for Microbiology, New York, NY, pp 544–550 (1987).
5 Baldet P, Gerbling H, Axiotis S and Douce R, Biotin biosynthesis in plants: identification of intermediates. *Eur J Biochem* **217**:479–485 (1993).
6 Patton DA, Johnson M and Ward ER, Biotin synthase from *Arabidopsis thaliana*. *Plant Physiol* **112**:371–378 (1996).
7 Shellhammer J and Meinke D, Arrested embryos from the *bio1* auxotroph of *Arabidopsis thaliana* contain reduced levels of biotin. *Plant Physiol* **110**:1021–1028 (1990).
8 Patton DA, Volrath S and Ward ER, Complementation of the *bio1 Arabidopsis* biotin auxotroph with a bacterial biotin biosynthetic gene. *Mol Gen Genet* **251**:261–266 (1996).
9 Patton DA, Schetter AL, Franzmann LH, Nelson K, Ward ER and Meinke DW, An embryo-defective mutant of *Arabidopsis* disrupted in the final step of biotin synthesis. *Plant Physiol* **116**:935–946 (1998).
10 Krell K and Eisenberg MA, The purification and properties of dethiobiotin synthetase. *J Biol Chem* **245**:6558–6566 (1970).
11 Huang W, Lindqvist Y, Schneider G, Gibson KJ, Flint D and Lorimer G, Crystal structure of an ATP-dependent carboxylase, dethiobiotin synthetase, at 1.65 Å resolution. *Structure* **2**:407–414 (1994).
12 Alexeev D, Bury SM, Boys CWG, Turner MA, Sawyer L, Ramsey AJ, Baxter HC and Baxter RL, Sequence and crystallization of *Escherichia coli* dethiobiotin synthetase, the penultimate enzyme of biotin biosynthesis. *J Mol Biol* **235**:774–776 (1994).
13 Gibson KJ, Lorimer GH, Rendina AR, Taylor WS, Cohen G, Gatenby AA, Payne WG, Roe DC, Lockett BA, Nudelman A, Marcovici D, Nachum A, Wexler BA, Marsilii EL, Turner IM, Howe LD, Kalbach CE and Chi H, Dethiobiotin synthetase: the carbonylation of 7,8-diaminononanoic acid proceeds regiospecifically via the N7-carbamate. *Biochemistry* **34**:10976–10984 (1995).
14 Yang G, Sandalova T, Lohman K, Lindqvist Y and Rendina AR, Active site mutants of *Escherichia coli* dethiobiotin synthetase: effects of mutations on enzyme catalytic and structural properties. *Biochemistry* **36**:4751–4760 (1997).
15 Huang W, Jia J, Gibson KJ, Taylor WS, Rendina AR, Schneider G and Lindqvist Y, Mechanism of an ATP-dependent carboxylase, dethiobiotin synthetase, based on crystallographic studies of complexes with substrates and a reaction intermediate. *Biochemistry* **34**:10985–10995 (1995).
16 Baxter RL and Baxter HC, Mechanism of *Escherichia coli* dethiobiotin synthetase – closure of the ureido ring of dethiobiotin involves formation of a carbamic phosphate mixed anhydride. *J Chem Soc Chem. Commun* 759–760 (1994).
17 Alexeev D, Baxter RL and Sawyer L, Mechanistic implications and family relationships from the structure of dethiobiotin synthetase. *Structure* **15**:1061–1072 (1994).
18 Alexeev D, Baxter RL, Smekal O and Sawyer L, Substrate binding and carboxylation by dethiobiotin synthetase-a kinetic and X-ray study. *Structure* **3**:1207–1215 (1995).
19 Gibson KJ, Isolation and chemistry of the mixed anhydride intermediate in the reaction catalyzed by dethiobiotin synthetase. *Biochemistry* **36**:8474–8478 (1997).
20 Kack H, Gibson KJ, Lindqvist Y and Schneider G, Snapshot of a phosphorylated substrate intermediate by kinetic crystallography. *Proc Natl Acad Sci USA* **95**:5495–5500 (1998).
21 Rendina A, Taylor W, Rayner D, Lockett B, Gibson K, Nudelman A, Marsilii E, Chi H and Yang G, Kinetic mechanism and alternate substrates for *Escherichia coli* dethiobiotin synthetase (DTBS). *The FASEB J* **11**:A1319 (1997).
22 Taylor W, Rendina A, Rayner D, Lockett B, Kranis K, Marsilii E, Chi H, Wawrzak Z, Calabrese J, Huang W, Jia J, Schneider G and Lindqvist Y, Inhibition of *Escherichia coli* dethiobiotin synthetase by stable phosphorus analogs of the carbamate intermediate. *The FASEB J* **11**:A1319 (1997).
23 Maracovici D, Synthesis of biotin, biotin vitamers and analogs. *PhD Thesis*, Bar Ilan University, Ramat Gan, Israel (1995).
24 Nudelman A, Biotin, Approaches to total synthesis and inhibitors of biotin biosynthesis. *PhD Thesis*, Bar Ilan University, Ramat Gan, Israel (1997).
25 Nudelman Ay, Nudelman Ab, Marcovici-Mizrahi D and Flint D, The synthesis of the vitamers of biotin. *Bioorganic Chem* (in press).
26 Somerville, CR and Ogren WL, Isolation of photorespiration mutants in *Arabidopsis thaliana*, in *Methods in Chloroplast Molecular Biology*, ed by Edelman M, Hallick RB and Chua N-H, Elsevier Biomedical, Amsterdam. pp 129–138 (1982).
27 Henderson SA, O'Conner J, Rendina AR, Savage GP and Simpson GW, The synthesis and biological activity of 'crippled biotin'. *Aust J Chem* **48**:1907–1916 (1995).
28 Lea PJ and Ridley SM, Glutamine synthetase and its inhibition, in *Herbicide and Plant Metabolism*, ed. by Dodge AD, Soc Exp Biol Seminar Series 38, Cambridge University Press, Cambridge. pp 137–170 (1989) and references therein.
29 Johnson CR, Boettcher BR, Cherpeck RE and Dolson MG, Design and synthesis of potent inhibitors of glutamine synthetase: 1. Cyclic analogs of phosphinothricin. *Bioorg Chem* **18**:154–159 (1990).
30 Logusch EW, Walker DM, McDonald JF and Franz JE, Inhibition of plant glutamine synthetases by substituted phosphinothricins. *Plant Physiol* **95**:1057–1062 (1991).
31 Abell LM and Villafranca JJ, Investigation of the mechanism of phosphinothricin inactivation of *Escherichia coli* glutamine synthetase using rapid quench kinetic techniques. *Biochemistry* **30**:6135–6141 (1991).
32 Liaw S-H and Eisenberg D, Structural model for the reaction mechanism of glutamine synthetase, based on five crystal structures of enzyme-substrate complexes. *Biochemistry* **33**:675–681 (1994).
33 Duncan K and Walsh CT, ATP-dependent inactivation and slow binding inhibition of *Salmonella typhimurium* D-alanine : D-alanine ligase (ADP) by (aminoalkyl)phosphinate and aminophosphonate analogues of D-alanine. *Biochemistry* **27**:3709–3714 (1988).
34 Fan C, Moews PC, Walsh CT and Knox JR, Vancomycin resistance: structure of D-alanine : D-alanine ligase at 2.3 Å resolution. *Science* **266**:439–443 (1994).
35 Hiratake J, Kato H and Oda J, Mechanism-based inactivation of glutathione synthetase by phosphinic acid transition-state analogue. *J Am Chem Soc* **116**:12059–12060 (1994).
36 Katoh M, Hiratake J, Kato H and Oda J, Mechanism-based inactivation of *E. coli* γ-glutamylcysteine synthetase by phosphinic acid- and sulfoximine-based transition-state analogues. *Bioorg Med Chem Lett* **6**:1437–1442 (1996).